Journal of Zhejiang University-SCIENCE A (Applied Physics & Engineering)
ISSN 1673-565X (Print); ISSN 1862-1775 (Online)
www.jzus.zju.edu.cn; www.springerlink.com
E-mail: jzus@zju.edu.cn

# Optimal design of prefabricated vertical drain-improved soft ground considering uncertainties of soil parameters*

Hong-yue SUN[1], Jun WANG[1], Dong-fei WANG[1], Yang YU[†‡1], Zhen-lei WEI[2]

[1]*Ocean College, Zhejiang University, Zhoushan 316021, China*

[2]*College of Civil Engineering and Architecture, Zhejiang University, Hangzhou 310058, China*

[†]E-mail: yang-yu@zju.edu.cn

Received June 2, 2019; Revision accepted Dec. 2, 2019; Crosschecked Dec. 12, 2019

**Abstract:** Prefabricated vertical drains (PVDs) are widely used to accelerate the consolidation process within soft ground. The overall degree of consolidation (DOC) of soft ground is highly dependent on the arrangement of PVDs, such as their length and spacing. Nevertheless, only the ranges of spacing and length are recommended in codes and standards, which renders it difficult for designers to determine the appropriate arrangement of PVDs. A method is proposed in this paper to determine the appropriate arrangement of PVDs based upon multiple objectives, such as cost, safety, and design robustness. In this method, the design robustness is evaluated by the signal-to-noise ratio of the overall DOC, which is determined using Monte-Carlo simulation based on the statistics of uncertain soil parameters. A framework is proposed based on the optimal procedure and illustrated with an example. The results indicate that the proposed method can determine the most preferred arrangement of PVDs. Additionally, compared with the traditional deterministic method, it can suggest a series or a unique optimal design when the uncertainties of soil parameters are considered. Furthermore, factors affecting the most preferred arrangement are discussed.

**Key words:** Robust geotechnical design; Consolidation; Prefabricated vertical drain (PVD) arrangement; Ground improvement
https://doi.org/10.1631/jzus.A1900227 **CLC number:** TU46

## 1 Introduction

Soft ground is widely spread not only on land, but also in coastal regions (Chen et al., 2016; Zheng et al., 2017; Yuan et al., 2018). For the safety of infrastructures built on soft ground, prefabricated vertical drains (PVDs) are widely used to accelerate the consolidation process by shortening the drainage path and accelerating the dissipation of excess pore water pressure within the soft ground (Bergado et al., 1991, 1993, 2002; Parsa-Pajouh et al., 2016; Kim et al., 2018a, 2018b; Nguyen et al., 2018), which is defined as PVD-improved soft ground. On PVD-improved soft ground, the safety of infrastructures such as embankments, foundations, and roads depends on the settlement and strength of the improved soft ground. Such an improvement is highly dependent on the design of PVDs (e.g. length and spacing). However, in practice, the length and spacing of PVDs are often selected by the designer according to the ranges of length and spacing of PVDs recommended in codes and standards, e.g. JGJ 79-2002 (MOC, 2002). The designer's experience becomes the dominant factor affecting the design effectiveness of PVDs. In addition, uncertainties in soil parameters render it more difficult to select an appropriate design

‡ Corresponding author

* Project supported by the National Natural Science Foundation of China (No. 41807224), the Zhejiang Provincial Natural Science Foundation of China (No. LQ17D020001), and the Joint Fund between Zhoushan City and Ocean College of Zhejiang University (No. 2017C82220), China

ORCID: Yang YU, https://orcid.org/0000-0001-8021-4401

of PVDs. Consequently, a method facilitating designers to determine the appropriate design of PVDs must be established, especially when the uncertainties of the soil parameters are considered.

The length and spacing of PVDs are two key design parameters. For the length of PVDs, full penetration is recommended in codes and standards to increase the drainage capacity of subsoil to the maximum (MOC, 2002). However, full penetration is uneconomic when the soil layer is thick (Ong et al., 2012), and it is also ineffective for a two-way drainage deposit with vacuum pressure owing to the vacuum pressure leakage (Geng et al., 2011). Hence, PVDs are partially penetrated into soil layer in practice. The spacing between PVDs is another important parameter in the design of PVD-improved ground. A large spacing may cause ineffectiveness of horizontal drainage, while a small spacing may increase the number of PVDs, which results in a high cost. Currently, the length and spacing of PVDs are primarily determined based on a trial-and-error approach utilizing some deterministic consolidation theories (Ho et al., 2015; Vu, 2015; Zhou et al., 2017; Li et al., 2018; Zou et al., 2018). Although such deterministic methods can be used to select the optimal design of PVDs, the unique optimal design of PVDs is difficult to determine if the uncertainties of soil parameters are considered.

Hence, Juang and his co-authors (Juang and Wang, 2013; Gong et al., 2014, 2016; Juang et al., 2014; Khoshnevisan et al., 2014) proposed the framework of robust geotechnical design (RGD). In the framework of RGD, input parameters are characterized as design parameters and noise factors. A robust design, which is insensitive to the variation in noise factors, can be obtained by adjusting the design parameters. In addition, multiobjectives such as safety, robustness, and cost can be simultaneously considered in RGD. The RGD has been used to optimize the designs of tunnels, slopes, and foundations (Gong et al., 2014, 2016; Juang et al., 2014; Yu et al., 2019). Based on these applications, the RGD has been proven appropriate to optimize the designs in geotechnical engineering with significant uncertainties in soil parameters. The concept of RGD is consistent with the objective of determining an optimal, reliable, and cost-efficient design of PVD-improved soft ground; hence, it can be an alternative option for optimizing PVDs for improving soft ground.

In this study, a method is proposed to determine the appropriate length and spacing of PVDs accounting for the uncertainties of soil parameters based on the concept of RGD. The overall degree of consolidation (DOC) after a certain amount of elapsed time is estimated by the settlement of the soil layer. Based on the overall DOC, the design robustness is evaluated and used to identify the optimal length and spacing of PVDs. A framework is established based on the optimal procedure and illustrated with an example. The most preferred PVD arrangement (e.g. the length and spacing) is determined based on the results of this study. Furthermore, the factors affecting the optimal PVD arrangement are discussed.

## 2 Methodology

### 2.1 Deterministic method to evaluate the overall DOC

The time-dependent settlement is often used to evaluate the overall DOC. Fig. 1 shows an embankment on a soft clay foundation treated with PVDs, which is adopted in this study as an illustrative example.

To evaluate the time-dependent settlement, the filling loading-influenced depth, $z_a$, is determined based on the following principle (MOC, 2002):

$$\frac{\sigma_{vz}}{\sigma_z} \geq 0.1, \tag{1}$$

where $\sigma_{vz}$ is the effective stress along the depth of a soil layer that is determined according to the bulk density of the soil stratum, $z_a$, and groundwater location; $\sigma_z$ is the additional stress induced by the filling loading on the subsoil surface. $\sigma_z$ is computed according to Boussinesq equations with respect to $z_a$ and the foundation width.

The soil foundation is divided into a number of sublayers. For each sublayer, the settlement is calculated according to the compression curve of soil deposit (Terzaghi, 1944; Terzaghi et al., 1996). Subsequently, the ultimate consolidation settlement $s_c$ can

be obtained by adding up the settlement of each sublayer. Based on different consolidation states, the computational procedure is expressed as follows.

If the $i$th sublayer is composed of under-consolidation soil $\sigma_{vzi}>\sigma_{pzi}$ or normally consolidation soil $\sigma_{vzi}=\sigma_{pzi}$, the settlement $s_c$ can be obtained as follows:

$$s_c=\sum_{i=1}^{\infty}\frac{H_i}{1+e_{0i}}\left(C_{ci}\lg\frac{\sigma_{zi}+\sigma_{vzi}}{\sigma_{vzi}}\right). \tag{2a}$$

If the $i$th sublayer is composed of over-consolidation soil ($\sigma_{vzi}<\sigma_{pzi}$), the settlement $s_c$ can be obtained as follows:

$$s_c=\sum_{i=1}^{\infty}\frac{H_i}{1+e_{0i}}\left(C_{ri}\lg\frac{\sigma_{pzi}}{\sigma_{vzi}}+C_{ci}\lg\frac{\sigma_{zi}+\sigma_{vzi}}{\sigma_{pzi}}\right), \quad \sigma_{zi}+\sigma_{vzi}>\sigma_{pzi}, \tag{2b}$$

$$s_c=\sum_{i=1}^{\infty}\frac{H_i}{1+e_{0i}}\left(C_{ri}\lg\frac{\sigma_{zi}+\sigma_{vzi}}{\sigma_{vzi}}\right), \quad \sigma_{zi}+\sigma_{vzi}\le\sigma_{pzi}. \tag{2c}$$

In Eqs. (2a)–(2c), $H_i$ is the thickness of the $i$th sublayer; $e_{0i}$ is the initial void ratio of soil in the $i$th sublayer; $C_{ci}$ and $C_{ri}$ are compression and recompression indices of the $i$th sublayer, respectively; $\sigma_{vzi}$, $\sigma_{zi}$, and $\sigma_{pzi}$ are the average effective stress, average additional stress, and pre-consolidation stress of the $i$th sublayer, respectively.

Because the PVDs are partially penetrated into the soil, the whole soil layer is divided into sublayers with and without PVDs, as shown in Fig. 1. For the sublayers without PVDs, the time-dependent settlement is predicted with the 1D consolidation theory proposed by Terzaghi (1944) and Terzaghi et al. (1996):

$$U_v=1-8\sum_{i=1}^{\infty}\frac{\exp\{-A_i^2c_vt/[2(z_a-L)]^2\}}{A_i^2}, \tag{3}$$

where $U_v$ is the DOC along the vertical direction; $A_i=(2i-1)\pi$ ($i$=1, 2, …); $t$ denotes the elapsed time; $L$ denotes the length of the PVD; $c_v$ represents the average vertical coefficient of consolidation along the whole thickness of soil layer. Therefore, the time-dependent settlement of soil sublayers without PVDs, $s_1(t)$, is expressed by

$$s_1(t)=U_vs_{c1}, \tag{4}$$

where $s_{c1}$ is the ultimate settlement of soil sublayers without PVDs calculated by Eq. (2).

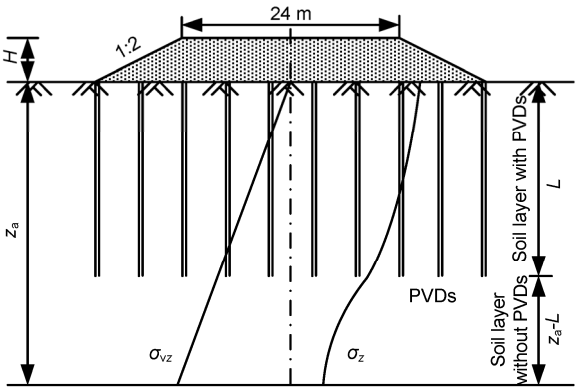


**Fig. 1 Embankment for calculation after Vu (2015)**
$H$ is the height of embankment

For the sublayers with PVDs, the axisymmetric consolidation solution proposed by Hansbo, which is called Hansbo's consolidation solution (Hansbo, 1979; Hansbo et al., 1981), is introduced to compute the time-dependent settlement for illustrative purposes. Additionally, other consolidation solutions can be used (Berry and Wilkinson, 1969; Rixner et al., 1986). Fig. 2 shows the computational unit cell for Hansbo's consolidation solution, in which a single PVD is contained in an axisymmetric soil model.

In the unit cell presented in Fig. 2, a one-way drainage deposit (pervious and impervious boundaries for top and bottom of the unit cell, respectively) is assumed in the unit cell. The average DOC of the unit cell can be divided into the DOCs along the radial and vertical directions (Carrillo, 1942), which can be expressed as follows:

$$U_{vh}=1-(1-U_v)(1-U_r), \tag{5}$$

where $U_{vh}$ and $U_r$ denote the average DOC and DOC along the radial direction, respectively. $U_v$ is derived by Eq. (3); $U_r$ is derived based upon the equal-strain assumption:

$$U_r = 1 - \exp\left[-\frac{2c_h t}{r_e^2 F(r_e)}\right], \tag{6}$$

$$F(r_e) = F_0(r_e) + F_s + F_r, \tag{7}$$

$$F_0(r_e) = \ln\left(\frac{r_e}{r_w}\right) - 0.75, \tag{8}$$

$$F_s = \ln\left(\frac{r_s}{r_w}\right)\left(\frac{k_h}{k_h'} - 1\right) = \ln(s)\left(\frac{k_h}{k_h'} - 1\right), \tag{9}$$

$$F_r = \frac{2\pi L^2}{3}\frac{k_h}{q_w}, \tag{10}$$

where $c_h$ denotes the horizontal coefficient of consolidation; $k_h$ and $k_h'$ represent the horizontal hydraulic conductivity of sublayers within the undisturbed and smear zones, respectively; $q_w$ denotes the vertical discharge capacity of the PVD; $r_e$, $r_s$, and $r_w$ represent the influenced radius, radius of smear zone, and equivalent radius of the PVD, respectively. $r_e$ is determined according to the PVD arrangement pattern (triangular or square) and PVD spacing ($D$), as shown in Fig. 3; $s$ is the ratio between $r_s$ and $r_w$.

For a band-shaped PVD, which is widely used in practice, the equivalent radius of a band-shaped PVD is $(a+b)/\pi$ (MOC, 2002), where $a$ and $b$ denote the width and thickness of a band-shaped PVD, respectively.

It is noteworthy that $F_0(r_e)$, $F_s$, and $F_r$ represent the effects of PVD arrangement pattern and spacing, smear effect, and well resistance on the consolidation behavior of PVD-improved soft ground. Many studies have been performed to investigate the effects of these expressions on the performance of PVDs (Rixner et al., 1986; Tran-Nguyen and Edil, 2011; Parsa-Pajouh et al., 2014; Azari et al., 2016). These three expressions are important for understanding the performance of PVDs in the design of PVD-improved soft ground.

Consequently, the time-dependent settlement of soil stratum with PVDs, $s_2(t)$, can be expressed:

$$s_2(t) = U_{vh} s_{c2}, \tag{11}$$

where $s_{c2}$ ($s_{c2}=s_c-s_{c1}$) is the ultimate settlement of the sublayers with PVDs.

Based on Eqs. (2), (4), and (11), the overall DOC of a specific design of PVDs in a particular soil layer, $U(\boldsymbol{d}, \boldsymbol{\theta})$, can be expressed as

$$U(\boldsymbol{d}, \boldsymbol{\theta}) = \frac{s_{c1}U_v + s_{c2}U_{vh}}{s_c}, \tag{12}$$

where $\boldsymbol{d}$ and $\boldsymbol{\theta}$ are the vectors for the design parameters and noise factors, respectively.

In the framework of RGD, the design parameters can be designated by the designer, and the noise factors cannot be fully eliminated. Therefore, in this paper, the vector of the design parameters is $\boldsymbol{d}=\{L, D\}$, and the vector of the noise factors can be $\boldsymbol{\theta}=\{c_h, c_v, k_h/k_h', k_h/q_w, s\}$. Because $c_h$ is determined according to $c_v$, $c=c_h/c_v$ is assumed as the noise factor instead of $c_h$. Therefore, the vector of the noise factors is rewritten as $\boldsymbol{\theta}=\{c, c_v, k_h/k_h', k_h/q_w, s\}$.

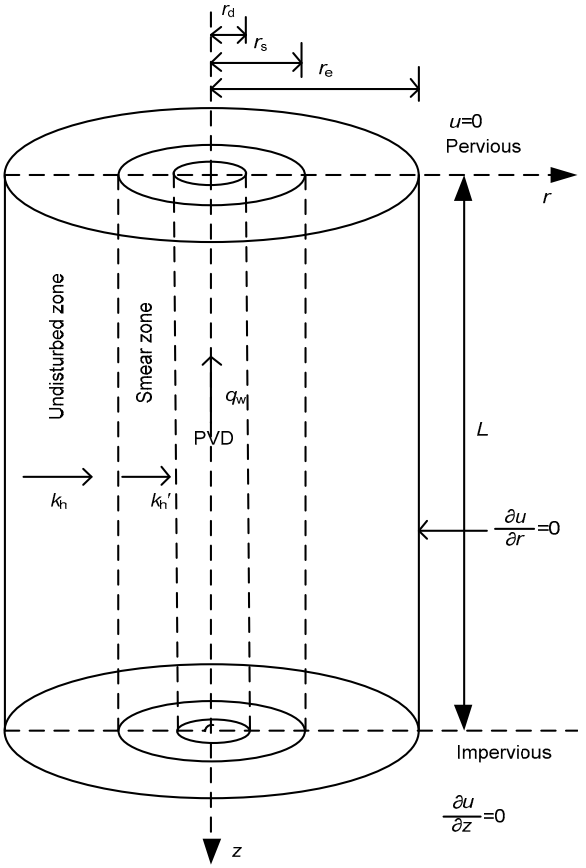


**Fig. 2 Axisymmetric consolidation unit cell with single PVD ($r_d$ is the equivalent radius of PVD; $u$ is the excess pore water pressure)**

## 2.2 Design robustness evaluation

Indices, including the signal-to-noise ratio (SNR), variation in response, feasibility robustness,

and the gradient of the system response, can be used to evaluate the design robustness. In this study, the SNR defined by Phadke (1989) is adopted not only because of its simplicity, but also because it can consider both the mean and standard deviation of the overall DOC. The SNR after a certain elapsed time since the installation of PVDs is expressed as

$$\mathrm{SNR}=10\lg\left(\frac{\bar{U}}{S_U}\right)^2, \tag{13}$$

where $\bar{U}$ and $S_U$ indicate the mean and standard deviation of the overall DOC, respectively. A higher SNR indicates that the overall DOC has a smaller variation regarding its mean and thus is less sensitive to noise factors.

The mean and standard deviation of the overall DOC can be obtained by the Monte-Carlo simulation (MCS) (Zhang et al., 2017; Wang et al., 2019). The MCS is used to generate random samples of noise factors based on their distribution, mean value, coefficient of variation (COV), and correlation coefficient. The MCS can provide a reliable estimation of the statistic features of the DOC. This study adopts the MCS to describe the statistic features of the DOC.

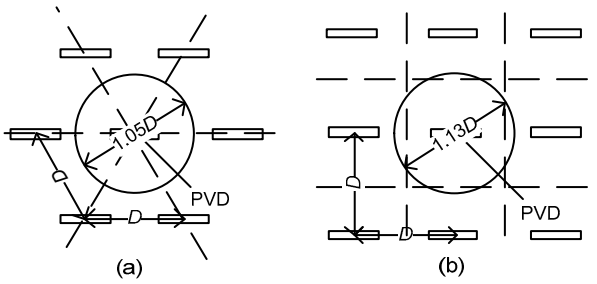


**Fig. 3 PVD arrangement patterns**
(a) Triangular; (b) Square

### 2.3 Cost estimation

The cost includes the labor cost, preloading material cost, and PVD material cost. The labor cost and preloading material cost are a function of the number of PVDs. This function is dictated by local experience and practice. For simplicity and illustrative purposes, the cost of using PVDs is assumed proportional to the length of PVDs and inversely proportional to the spacing between PVDs. Therefore, the expression proposed by Vu (2015) is introduced to estimate the cost $C$:

$$C=\frac{L}{D^2}. \tag{14}$$

## 3 Framework for selecting the most preferred design parameters

A flow chart to illustrate the framework for determining the most preferred design of PVDs is shown in Fig. 4. This framework can be summarized in the following steps:

Step 1: Define the problem and divide all input parameters into two groups: the design parameters and noise factors. Recall that the design parameters of PVD-improved soft clay ground are the length ($L$) and spacing ($D$) of PVDs. Further, the noise factors are the ratio between the horizontal and vertical consolidation coefficient ($c$), vertical consolidation coefficient ($c_v$), ratio between horizontal hydraulic conductivities in undisturbed and smear zone ($k_h/k_h'$), ratio between hydraulic conductivity in undisturbed zone and drainage capacity of the PVD ($k_h/q_w$), and ratio between radius of smear zone and equivalent radius of the PVD ($s$).

Step 2: Identify the range of design parameters and then characterize the uncertainties of the noise factors. The values of $L$ and $D$ are specified in discrete numbers based upon their typical ranges and arrangement patterns (triangular or square). The uncertainties in the noise factors are often quantified using the available data from site investigation and laboratory tests, and augmented with experiences or published literature.

Step 3: Identify the feasible design based on the computed overall DOC. For a specific PVD-improved soft ground, effective and additional stresses are obtained based on the magnitude of preloading or loading determined according to codes and standards (MOC, 2002). For each PVD design, the mean value of the overall DOC obtained by the MCS is the mean overall DOC of 10 000 samples. If the computed mean value of the overall DOC is larger than the target overall DOC, then the PVD

design is feasible. Repeat this computational procedure for all the PVD designs, which completes the loop in Fig. 4.

Step 4: Compute the cost and design robustness for each feasible design. Subsequently, the preferred designs of PVDs can be obtained based on the Pareto front and knee point, which can be determined according to the relationships of cost and design robustness, as shown in Fig. 5. The detailed procedures (Deb et al., 2002; Deb and Gupta, 2011; Khoshnevisan et al., 2014) to establish the Pareto front and knee point are described subsequently.

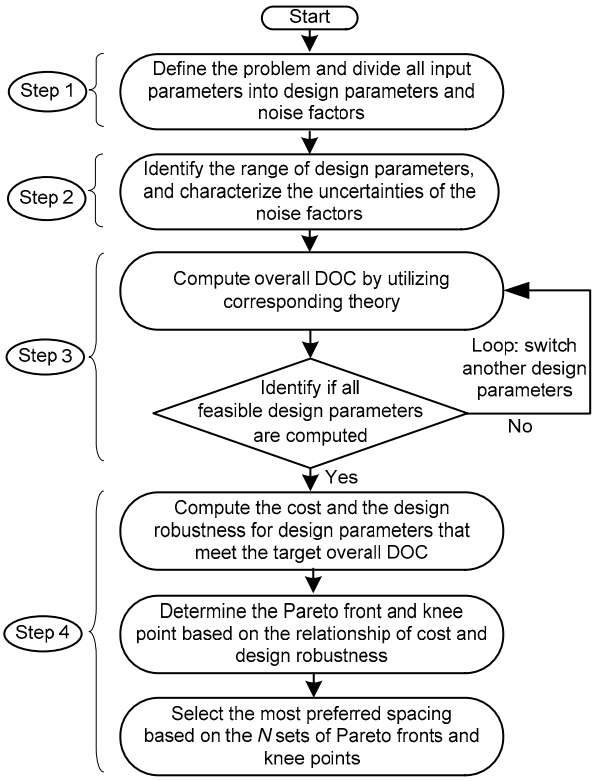


**Fig. 4 Flowchart of the proposed method**

## 4 Illustrative example

### 4.1 Characterization of design parameters and noise factors

A PVD-improved soft clay ground (Fig. 1), reported by Vu (2015), is introduced to illustrate the application of the proposed method and framework. The soil properties are listed in Table 1, where $\gamma_i$ is the unit weight of the $i$th sublayer. The embankment is

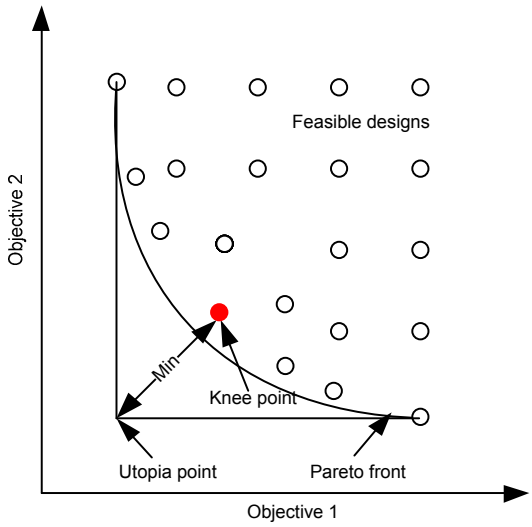


**Fig. 5 Schematic diagram of the principle of robust geotechnical design (Juang et al., 2014)**

24 m wide and 6 m high. The slope of the embankment is 1:2. The bulk density of the fill material is 20 kN/m$^3$. The underground water level is located 1.0 m below the subsoil surface. The target overall DOC is assumed to be 90% in one year ($t$=1 a) after the PVDs have been installed. The band-shaped PVD, whose geometric dimensions are 100 mm×5 mm, is installed with a triangular arrangement pattern.

The typical ranges of length and spacing of the PVDs are 1.0–32.0 m and 0.8–5.0 m, respectively (Vu, 2015). The length and spacing of the PVDs are selected with intervals of 1 m and 42 mm, respectively. Therefore, the length ($L$) is selected from {1.0, 2.0, 3.0, …, 32.0} m, and the spacing ($D$) from {0.8, 0.842, 0.884, …, 5.0} m. Combining $L$ and $D$, the total number of all designs is 3232.

Recall that $c$, $c_h$, $k_h/k_h'$, $k_h/q_w$, and $s$ are the noise factors. The overall DOC is sensitive to these noise factors, which are significantly uncertain. The mean and COV of these noise factors are evaluated based on published literature. The coefficient of vertical consolidation ($c_v$) varies between 5.2 and 14.2 m$^2$/a (Leclair, 1988), and the magnitude of $c$ varies between 1.78 and 2.70 (Heo and Bae, 2013). Further, the noise factor of $k_h/k_h'$ varies between 1.03 and 1.25, and the noise factor of $s$ varies between 3 and 4 (Tran-Nguyen and Edil, 2011). The typical range of $k_h/q_w$ is $2.1\times10^{-3}$–$4.2\times10^{-3}$ m$^{-2}$ (Chai and Miura, 1999). Based on these values, the mean and standard deviation of the noise factors are evaluated based on

the following equations (Duncan, 2000; Cherubini et al., 2001):

$$\mu = \frac{\max + \min}{2}, \tag{15}$$

$$\sigma = \frac{\max - \min}{4}, \tag{16}$$

$$\mathrm{COV} = \frac{\sigma}{\mu}, \tag{17}$$

where $\mu$ and $\sigma$ represent the mean and standard deviation of each noise factor, respectively; max and min denote the maximum and minimum values of each noise factor, respectively. The obtained mean values and standard deviations of the noise factors are summarized in Table 2.

### 4.2 Selection of the preferred PVD designs based on Pareto front and knee point

For the illustrative example shown in Fig. 1, the influenced depths ($z_a$) and ultimate consolidation settlement ($s_c$) are calculated as 65.7 m and 2.31 m, respectively. For each of the 3232 designs, the MCS is used to calculate the overall DOC. The detailed statistics of the noise factors are listed in Table 2. To determine the appropriate sample size, variations in the mean overall DOC of the PVD design ($L$=32 m, $D$=5 m) were computed with different sample sizes. Fig. 6 shows that the variations in the mean overall DOC tend to be stable at $N$=10 000. Therefore, a sample size of $N$=10 000 was used for each candidate design in MCS. If the mean of the calculated overall DOC is not less than 90%, then this PVD design is feasible. Repeating this computational procedure, the feasible designs obtained by the MCS are shown in Fig. 7.

Obtaining the optimal design in terms of robustness and cost is the goal of RGD. For each feasible design, its cost and robustness can be obtained. However, the design with the lowest cost and the highest robustness, which is called the utopia point, is generally unattainable because the two objectives, cost and roughness, are typically incompatible (Khoshnevisan et al., 2014). The nondominated designs form the Pareto front, which reveals a tradeoff between the two objectives (Deb et al., 2002). The knee point is used to identify the optimal designs in the Pareto front, which is the point that is the nearest from the utopia point (Khoshnevisan et al., 2014).

Based on the feasible designs in Fig. 7 and the method proposed by Khoshnevisan et al. (2014), the Pareto front can be obtained by dividing the cost into many sublevels. Within each sublevel, the PVD design that has the largest SNR is selected. All the PVD designs selected from each cost sublevel compose the Pareto front. As shown in Fig. 7, the PVD designs on the Pareto front are nondominant designs, where one PVD design is not superior to another on both objectives of cost and robustness. The Pareto front provides the designer with a series of optimal designs, which can be selected based on the

**Table 1 Soil properties of the illustrative example in Fig. 1**

| Layer | $H_i$ (m) | $\gamma_i$ (kN/m$^3$) | $e_{0i}$ | $C_{ci}$ | $C_{ri}$ | $\sigma_{pzi}$ (kPa) | $c_v$ (m$^2$/a) |
|---|---|---|---|---|---|---|---|
| 1 | 31.7 | 16.1 | 1.67 | 0.627 | 0.030 | 66 | 8.31 |
| 2 | 1.9 | 15.7 | 1.75 | 0.469 | 0.061 | 86 | 10.30 |
| 3 | >7.0 | 15.7 | 1.75 | 0.138 | 0.016 | 125 | 27.63 |

Note: Layer 1 is silty clay with a high plasticity state; Layer 2 is silty clay with a plasticity state; Layer 3 is clay with a stiff plasticity state

**Table 2 Statistics of the noise factors**

| Item | $c$ | $c_v$ (m$^2$/a) | $k_h/k_h'$ | $k_h/q_w$ ($\times10^{-3}$ m$^{-2}$) | $s$ |
|---|---|---|---|---|---|
| Range | 1.78–2.70 | 5.2–14.2 | 1.03–1.25 | 2.1–4.2 | 3–4 |
| $\mu$ | 2.24 | 9.7 | 1.14 | 3.15 | 3.50 |
| $\sigma$ | 0.23 | 2.25 | 0.06 | 0.53 | 0.25 |
| COV | 0.10 | 0.232 | 0.05 | 0.17 | 0.07 |
| Distribution | Lognormal | Lognormal | Lognormal | Lognormal | Lognormal |

Note: Summarized according to the references (Leclair, 1988; Chai and Miura, 1999; Tran-Nguyen and Edil, 2011; Heo and Bae, 2013)

designated cost or robustness of the project. If neither the cost nor robustness is designated in a project, a single most preferred PVD design can be determined based on the knee point. To find the knee point, $L/D^2$ and SNR should be normalized using the following equation:

$$X_{\mathrm{N}}=\frac{x_i-x_{\min}}{x_{\max}-x_{\min}}, \tag{18}$$

where $X_{\mathrm{N}}$ represents the normalized value of $L/D^2$ and SNR; $x_i$, $x_{\min}$, and $x_{\max}$ denote the obtained output, the minimum output, and the maximum output, respectively.

In the coordinates of the normalized $L/D^2$ and SNR, the utopia point, which is the point with the lowest cost and highest robustness, is first obtained. It is noteworthy that the utopia point does not exist in reality. The knee point is determined as the point that has the minimum Eulerian distance to the utopia point. Fig. 7 illustrates the knee point of the PVD-improved soft clay ground. Compared with the PVD design obtained by Vu (2015), the length of the most preferred PVD design is approximately equal to that of Vu (2015)'s, and the spacing of the most preferred PVD design is approximately two-third the spacing of Vu (2015)'s. This means that the cost of the most preferred PVD design ($L/D^2$) in RGD is higher than that obtained using the deterministic method. More expense should be incurred to address the uncertainties of the soil parameters.

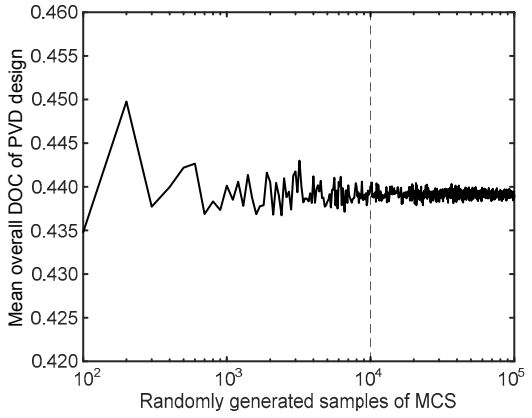


**Fig. 6 Effect of randomly generated samples of MCS on the variation of the mean overall DOC of PVD design (*L*=32 m, *D*=5 m)**

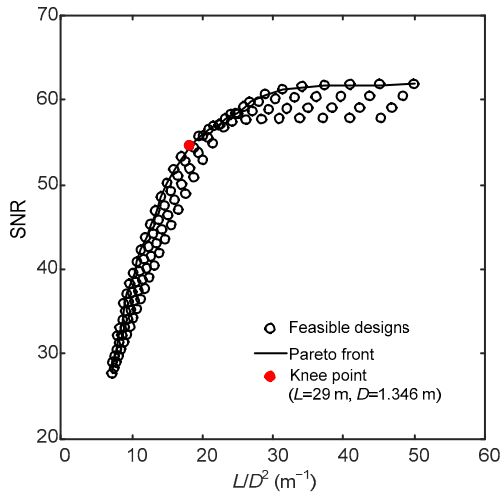


**Fig. 7 Feasible designs, Pareto front, and knee point of the illustrative example**

## 5 Discussion

### 5.1 Effect of target overall DOC on the preferred PVD design

To investigate the effects of different target overall DOCs on the preferred PVD arrangement, Pareto fronts and knee points with target overall DOCs of 85%, 90%, and 95% are obtained and presented in Fig. 8. When the cost ($L/D^2$) of the PVDs is less than 23 $m^{-1}$, the cost ($L/D^2$) of the PVDs increases with the target overall DOC (under the same SNR level). This means that higher safety requirements should be fulfilled with higher costs. When $L/D^2$ is sufficiently large (e.g. >23 $m^{-1}$), the robustness of the PVD design is not affected by the target overall DOC.

### 5.2 Effect of elapsed time on the preferred PVD design

Fig. 9 shows the Pareto fronts and knee points corresponding to the elapsed times of 1 a, 2 a, and 3 a. As shown, the cost of the most preferred PVD design at the knee point decreases as the elapsed time increases. However, a longer elapsed time means a lower constructional efficiency. Therefore, a higher constructional efficiency is guaranteed by a higher cost. For these three elapsed times, when the cost is sufficiently high, the design robustness reaches its maximum. This means that if $L/D^2$ is sufficiently large, the PVD design is fully robust against the

variation in the noise factors. Meanwhile, as $L/D^2$ decreases, PVD designs with shorter elapsed times cost more than those with longer elapsed times when the robustness is at the same level.

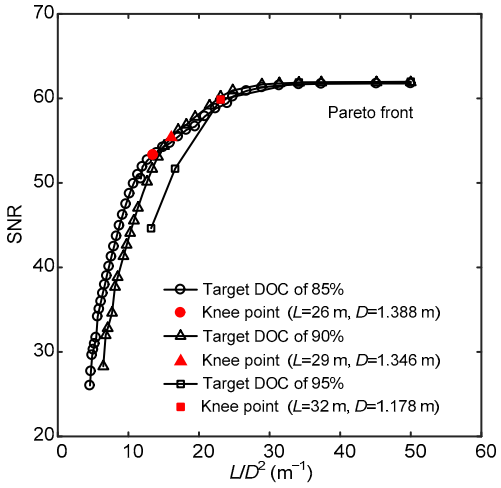


**Fig. 8 Pareto fronts and knee points with different target overall DOCs**

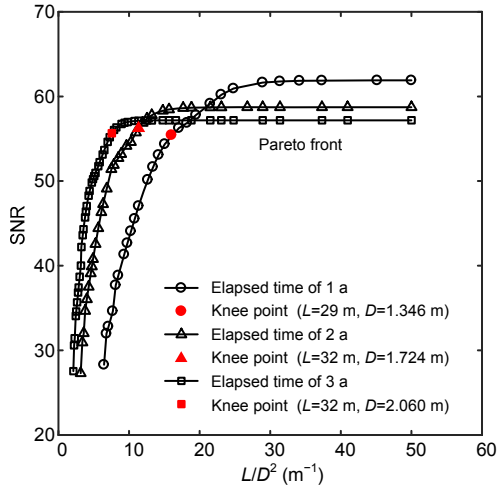


**Fig. 9 Pareto fronts and knee points with different elapsed times**

## 5.3 Effect of equivalent radius on the preferred PVD design

As recommended in the codes and standards (MOC, 2002), the equivalent radius of the band-shaped drain in the previous sections was calculated as $(a+b)/\pi$, which was initially proposed by Hansbo (Hansbo, 1979; Hansbo et al., 1981). Additionally, other equivalent rules exist for calculating the equivalent radius. To investigate the effects of different equivalent rules on the preferred PVD arrangement, the equivalent rule proposed by Rixner et al. (1986), $(a+b)/2$, is introduced as a comparison. Fig. 10 shows the Pareto fronts and knee points with equivalent rules proposed by Hansbo (1979), Hansbo et al. (1981), and Rixner et al. (1986). As shown, the optimal results are not affected by the equivalent rules because the two Pareto fronts and knee points almost coincide with each other.

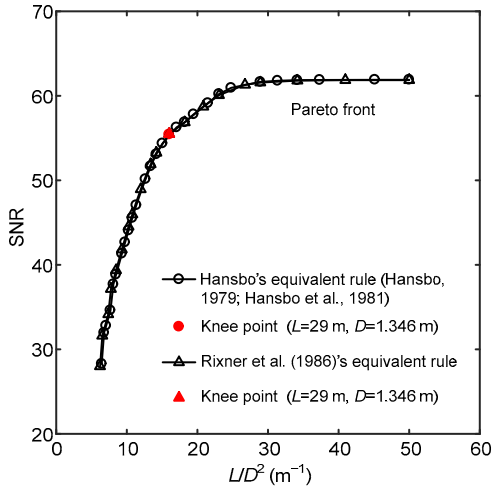


**Fig. 10 Pareto fronts and knee points with different equivalent rules**

## 5.4 Effects of different arrangement patterns of PVDs on the preferred PVD arrangement

Square and triangular (Fig. 3) are two typical patterns of PVDs. To investigate the effects of square and triangular patterns on the preferred PVD arrangement, Pareto fronts and knee points corresponding to these two patterns are obtained and presented in Fig. 11. As shown in Fig. 11, PVD designs with the triangular pattern are more robust than those with the square pattern. Therefore, the triangular pattern is suggested when addressing uncertainties in the soil parameters.

## 5.5 Effects of the coefficient of variation of noise factors on the preferred PVD design

The COV of noise factors may be different in different situations. The effects of different COVs on the preferred PVD arrangement is discussed in this section. Four sets of COVs (0.1, 0.2, 0.3, and 0.4)

were assumed for each noise factor. Fig. 12 shows the Pareto fronts and knee points with the assumed COVs. For noise factors $c$, $c_v$, and $k_h/q_w$, as the COV increases, the cost ($L/D^2$) increases and the SNR decreases. This means that the robustness decreases as the uncertainties of the noise factors increase. Higher COVs require higher costs ($L/D^2$). Therefore, if the actual COVs of $c$, $c_v$, and $k_h/q_w$ are underestimated, the cost of the most preferred PVD design will be underestimated. Furthermore, the robustness and cost are not sensitive to the variation in COVs for noise factors $k_h/k_h'$ and $s$.

### 5.6 Effects of correlations between noise factors on the preferred PVD design

Correlations may exist between noise factors in practical projects, which might affect the consolidation process. The effects of correlations between noise factors on the preferred PVD arrangement are discussed in this section. The correlations are analyzed using 10 combinations among the five noise factors. We analyzed the positive and negative correlations between these noise factors, owing to the lack of relevant research. Seven sets of correlation coefficients (−0.9, −0.6, −0.3, 0, 0.3, 0.6, and 0.9) were assumed for each combination. Table 3 shows the cost ($L/D^2$) of the most preferred PVD design at the knee point with different correlation coefficients. For most combinations, the correlations between noise factors do not affect the cost of the preferred PVD design. For combination [$c$, $c_v$], the cost increases with the correlation coefficients between them, which means that positive correlations between $c$ and $c_v$ require higher costs. For combinations [$c$, $k_h/q_w$] and [$c_v$, $k_h/q_w$], the cost decreases as the correlations between them increase, which means that negative correlations between them require higher costs. Fig. 13 shows the Pareto fronts and knee points with the assumed correlations for combinations [$c$, $c_v$] and [$c_v$, $k_h/q_w$]. For combination [$c$, $c_v$], as the correlation increases, the cost increases and the robustness decreases (when the correlation between them increases from −0.9 to 0.9, the SNR decreases from 55.85 to 53.67). Additionally, the robustness increases and the cost decreases as the correlation between $c_v$ and $k_h/q_w$ increases (when the correlation between them increases from −0.9 to 0.9, the SNR increases from 53.74 to 56.14). The results imply that the preferred PVD design might change considering the correlations between certain noise factors.

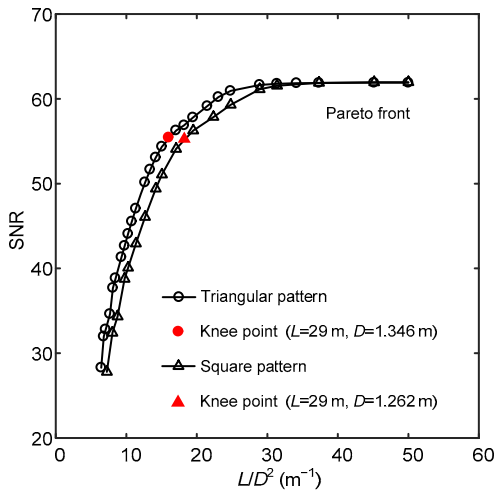


**Fig. 11 Pareto fronts and knee points with different arrangement patterns**

**Table 3 Cost of the most preferred PVD design with different correlation coefficients**

| Correlation coefficient | Cost ($L/D^2$) of the most preferred PVD design (m$^{-1}$) | | | | | | | | | |
|---|---|---|---|---|---|---|---|---|---|---|
| | [$c$, $c_v$] | [$c$, $k_h/k_h'$] | [$c$, $k_h/q_w$] | [$c$, $s$] | [$c_v$, $k_h/k_h'$] | [$c_v$, $k_h/q_w$] | [$c_v$, $s$] | [$k_h/k_h'$, $k_h/q_w$] | [$k_h/k_h'$, $s$] | [$k_h/q_w$, $s$] |
| −0.9 | 16.01 | 18.21 | 19.48 | 18.21 | 18.21 | 20.90 | 18.21 | 18.21 | 18.21 | 18.21 |
| −0.6 | 17.05 | 18.21 | 19.48 | 18.21 | 18.21 | 19.48 | 18.21 | 18.21 | 18.21 | 18.21 |
| −0.3 | 18.21 | 18.21 | 18.21 | 18.21 | 18.21 | 18.21 | 18.21 | 18.21 | 18.21 | 18.21 |
| 0 | 18.21 | 18.21 | 18.21 | 18.21 | 18.21 | 18.21 | 18.21 | 18.21 | 18.21 | 18.21 |
| 0.3 | 19.48 | 18.21 | 18.21 | 18.21 | 18.21 | 17.05 | 18.21 | 18.21 | 18.21 | 18.21 |
| 0.6 | 19.48 | 18.21 | 18.21 | 18.21 | 18.21 | 17.05 | 18.21 | 18.21 | 18.21 | 18.21 |
| 0.9 | 20.90 | 18.21 | 17.05 | 18.21 | 18.21 | 16.01 | 18.21 | 18.21 | 18.21 | 18.21 |

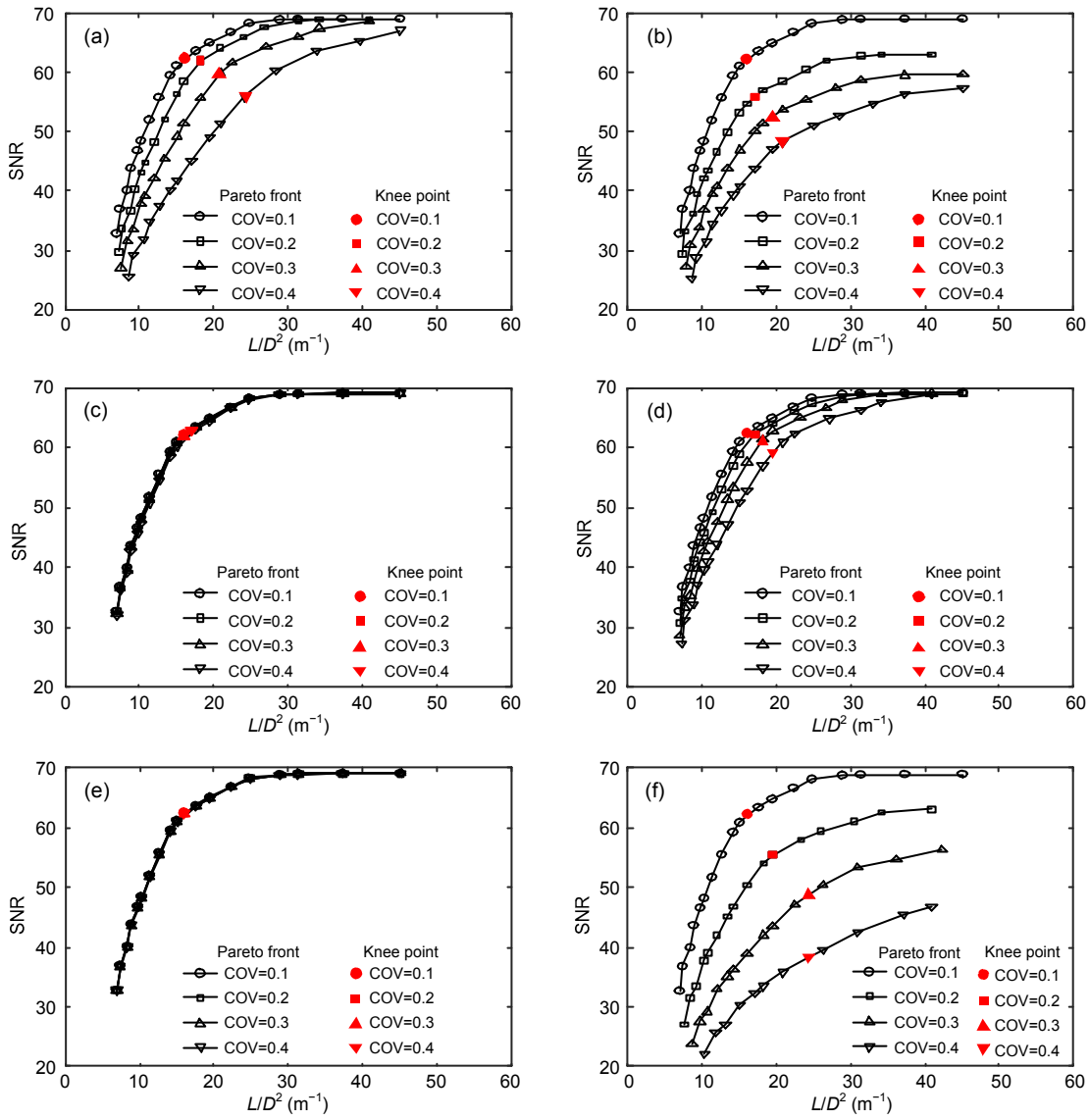


**Fig. 12 Pareto fronts and knee points with different COVs**

(a) $c$; (b) $c_v$; (c) $k_h/k_h'$; (d) $k_h/q_w$; (e) $s$; (f) All noise factors

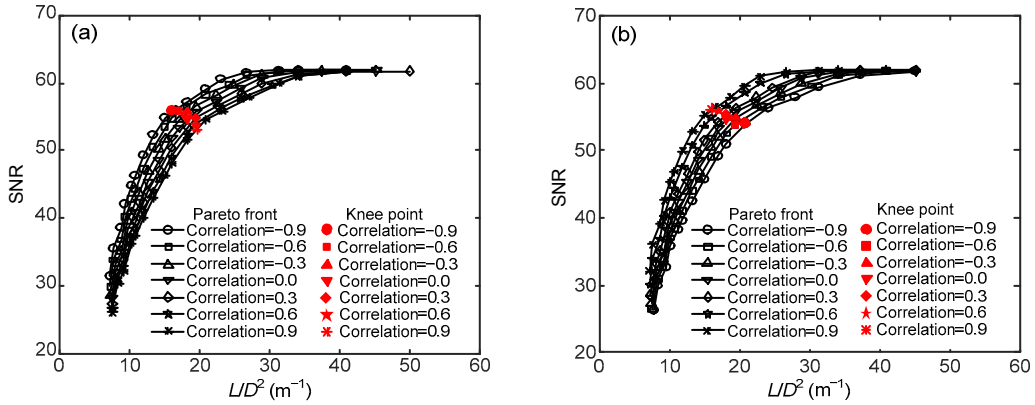


**Fig. 13 Pareto fronts and knee points with different correlations**

(a) $c$ and $c_v$; (b) $c_v$ and $k_h/q_w$

## 6 Conclusions

A method was proposed herein to determine the appropriate PVD arrangement based on an RGD. Both Hansbo's and Terzaghi's consolidation solutions were introduced to evaluate the overall DOC, based on which the design robustness was evaluated using the MCS. A framework was established based on the optimal procedure and illustrated with an example. The most preferred arrangement of PVDs was suggested based on the results of this study. Additionally, we discovered that the target overall DOC, elapsed time, and PVD arrangement pattern affected the optimal PVD design when the cost was in a lower range. However, these effects are negligible when the cost is sufficiently high, which means that higher costs can guarantee the design robustness of PVD-improved soft clay ground. Moreover, we discovered that the COVs and correlations of some noise factors affected the optimal PVD design. If the COVs of certain noise factors are underestimated, the cost of the most preferred PVD design will be underestimated.

### Contributors

Yang YU designed the research. Jun WANG, Dong-fei WANG, and Zhen-lei WEI processed the corresponding data and wrote the code. Hong-yue SUN and Jun WANG wrote the first draft of the manuscript. Hong-yue SUN and Yang YU revised and edited the final version.

### Conflict of interest

Hong-yue SUN, Jun WANG, Dong-fei Wang, Yang YU, and Zhen-lei WEI declare that they have no conflict of interest.

### Acknowledgements

The authors thanks for the Zhejiang Seaport Investment and Operation Group Co., Ltd., China for providing the project background of this study. The authors also want to express their commemoration of Dr. Gang WU (Zhejiang University, China), who helped to establish the theoretical model of this study.

### References

Azari B, Fatahi B, Khabbaz H, 2016. Assessment of the elastic-viscoplastic behavior of soft soils improved with vertical drains capturing reduced shear strength of a disturbed zone. *International Journal of Geomechanics*, 16(1):B4014001. https://doi.org/10.1061/(asce)gm.1943-5622.0000448

Bergado DT, Asakami H, Alfaro MC, et al., 1991. Smear effects of vertical drains on soft Bangkok clay. *Journal of Geotechnical Engineering*, 117(10):1509-1530. https://doi.org/10.1061/(asce)0733-9410(1991)117:10(1509)

Bergado DT, Alfaro MC, Balasubramaniam AS, 1993. Improvement of soft Bangkok clay using vertical drains. *Geotextiles and Geomembranes*, 12(7):615-663. https://doi.org/10.1016/0266-1144(93)90032-J

Bergado DT, Balasubramaniam AS, Fannin RJ, et al., 2002. Prefabricated vertical drains (PVDs) in soft Bangkok clay: a case study of the new Bangkok international airport project. *Canadian Geotechnical Journal*, 39(2):304-315. https://doi.org/10.1139/t01-100

Berry PL, Wilkinson WB, 1969. The radial consolidation of clay soils. *Géotechnique*, 19(2):253-284. https://doi.org/10.1680/geot.1969.19.2.253

Carrillo N, 1942. Simple two and three dimensional case in the theory of consolidation of soils. *Journal of Mathematics and Physics*, 21(1-4):1-5. https://doi.org/10.1002/sapm19422111

Chai JC, Miura N, 1999. Investigation of factors affecting vertical drain behavior. *Journal of Geotechnical and Geoenvironmental Engineering*, 125(3):216-226. https://doi.org/10.1061/(asce)1090-0241(1999)125:3(216)

Chen J, Shen SL, Yin ZY, et al., 2016. Evaluation of effective depth of PVD improvement in soft clay deposit: a field case study. *Marine Georesources & Geotechnology*, 34(5):420-430. https://doi.org/10.1080/1064119X.2015.1016638

Cherubini C, Christian JT, Baecher GB, et al., 2001. Factor of safety and reliability in geotechnical engineering. *Journal of Geotechnical and Geoenvironmental Engineering*, 127(8):700-721. https://doi.org/10.1061/(asce)1090-0241(2001)127:8(700)

Deb K, Gupta S, 2011. Understanding knee points in bicriteria problems and their implications as preferred solution principles. *Engineering Optimization*, 43(11):1175-1204. https://doi.org/10.1080/0305215X.2010.548863

Deb K, Pratap A, Agarwal S, et al., 2002. A fast and elitist multiobjective genetic algorithm: NSGA-II. *IEEE Transactions on Evolutionary Computation*, 6(2):182-197. https://doi.org/10.1109/4235.996017

Duncan JM, 2000. Factors of safety and reliability in geotechnical engineering. *Journal of Geotechnical and Geoenvironmental Engineering*, 126(4):307-316. https://doi.org/10.1061/(asce)1090-0241(2000)126:4(307)

Geng XY, Indraratna B, Rujikiatkamjorn C, 2011. Effectiveness of partially penetrating vertical drains under a combined surcharge and vacuum preloading. *Canadian Geotechnical Journal*, 48(6):970-983. https://doi.org/10.1139/t11-011

Gong WP, Wang L, Juang CH, et al., 2014. Robust geotechnical design of shield-driven tunnels. *Computers and Geotechnics*, 56:191-201. https://doi.org/10.1016/j.compgeo.2013.12.006

Gong WP, Juang CH, Khoshnevisan S, et al., 2016. *R*-LRFD: load and resistance factor design considering robustness. *Computers and Geotechnics*, 74:74-87.

https://doi.org/10.1016/j.compgeo.2015.12.017

Hansbo S, 1979. Consolidation of clay by band-shaped prefabricated drains. *Ground Engineering*, 12(5):16-25.

Hansbo S, Jamiolkowski M, Kok L, 1981. Consolidation by vertical drains. *Géotechnique*, 31(1):45-66. https://doi.org/10.1680/geot.1981.31.1.45

Heo Y, Bae W, 2013. A statistical evaluation of consolidation properties of marine clay in South Korea. *Marine Georesources & Geotechnology*, 31(3):209-224. https://doi.org/10.1080/1064119X.2012.661030

Ho L, Fatahi B, Khabbaz H, 2015. A closed form analytical solution for two-dimensional plane strain consolidation of unsaturated soil stratum. *International Journal for Numerical and Analytical Methods in Geomechanics*, 39(15): 1665-1692. https://doi.org/10.1002/nag.2369

Juang CH, Wang L, 2013. Reliability-based robust geotechnical design of spread foundations using multi-objective genetic algorithm. *Computers and Geotechnics*, 48:96-106. https://doi.org/10.1016/j.compgeo.2012.10.003

Juang CH, Wang L, Hsieh HS, et al., 2014. Robust geotechnical design of braced excavations in clays. *Structural Safety*, 49:37-44. https://doi.org/10.1016/j.strusafe.2013.05.003

Khoshnevisan S, Gong WP, Wang L, et al., 2014. Robust design in geotechnical engineering–an update. *Georisk: Assessment and Management of Risk for Engineered Systems and Geohazards*, 8(4):217-234. https://doi.org/10.1080/17499518.2014.980274

Kim YT, Nguyen BP, Yun DH, 2018a. Analysis of consolidation behavior of PVD-improved ground considering a varied discharge capacity. *Engineering Computations*, 35(3):1183-1202. https://doi.org/10.1108/EC-06-2017-0199

Kim YT, Nguyen BP, Yun DH, 2018b. Effect of artesian pressure on consolidation behavior of drainage-installed marine clay deposit. *Journal of Materials in Civil Engineering*, 30(8):04018156. https://doi.org/10.1061/(asce)mt.1943-5533.0002344

Leclair DG, 1988. Prediction of Embankment Performance Using In-situ Tests. MS Thesis, University of British Columbia, Vancouver, Canada.

Li YC, Tong X, Chen Y, et al., 2018. Non-monotonic piezocone dissipation curves of backfills in a soil-bentonite slurry trench cutoff wall. *Journal of Zhejiang University-SCIENCE A (Applied Physics & Engineering)*, 19(4): 277-288. https://doi.org/10.1631/jzus.A1700097

MOC (Ministry of Construction of the People's Republic of China), 2002. Technical Code for Ground Treatment of Buildings, JGJ 79-2002. National Standards of People's Republic of China (in Chinese).

Nguyen BP, Yun DH, Kim YT, 2018. An equivalent plane strain model of PVD-improved soft deposit. *Computers and Geotechnics*, 103:32-42. https://doi.org/10.1016/j.compgeo.2018.07.004

Ong CY, Chai JC, Hino T, 2012. Degree of consolidation of clayey deposit with partially penetrating vertical drains. *Geotextiles and Geomembranes*, 34:19-27. https://doi.org/10.1016/j.geotexmem.2012.02.008

Parsa-Pajouh A, Fatahi B, Vincent P, et al., 2014. Trial embankment analysis to predict smear zone characteristics induced by prefabricated vertical drain installation. *Geotechnical and Geological Engineering*, 32(5):1187-1210. https://doi.org/10.1007/s10706-014-9789-9

Parsa-Pajouh A, Fatahi B, Khabbaz H, 2016. Experimental and numerical investigations to evaluate two-dimensional modeling of vertical drain-assisted preloading. *International Journal of Geomechanics*, 16(1):B4015003. https://doi.org/10.1061/(asce)gm.1943-5622.0000507

Phadke MS, 1989. Quality engineering using design of experiments. *In*: Dehnad K (Ed.), Quality Control, Robust Design, and the Taguchi Method. Springer, Boston, USA, p.31-50.

Rixner JJ, Kraemer SR, Smith AD, 1986. Prefabricated Vertical Drains: Engineering Guidelines. Federal Highway Administration, Washington DC, USA.

Terzaghi K, 1944. Theoretical Soil Mechanics. Chapman and Hali Ltd., John Wiler and Sons, Inc., New York, USA.

Terzaghi K, Peck RB, Mesri G, 1996. Soil Mechanics in Engineering Practice, 3rd Edition. John Wiley & Sons, New York, USA.

Tran-Nguyen HH, Edil TB, 2011. The characteristics of PVD smear zone. *In*: Han J, Alzamora DE (Eds.), Geo-frontiers 2011: Advances in Geotechnical Engineering. ASCE, Dallas, USA, p.748-757. https://doi.org/10.1061/41165(397)77

Vu VT, 2015. Optimal layout of prefabricated vertical drains. *International Journal of Geomechanics*, 15(3):06014020. https://doi.org/10.1061/(asce)gm.1943-5622.0000434

Wang Z, Yu Y, Sun HY, et al., 2019. Robust optimization of the constructional time delay in the design of double-row stabilizing piles. *Bulletin of Engineering Geology and the Environment*. https://doi.org/10.1007/s10064-019-01554-7

Yu Y, Shen MF, Sun HY, et al., 2019. Robust design of siphon drainage method for stabilizing rainfall-induced landslides. *Engineering Geology*, 249:186-197. https://doi.org/10.1016/j.enggeo.2019.01.001

Yuan XQ, Wang Q, Lu WX, et al., 2018. Indoor simulation test of step vacuum preloading for high-clay content dredger fill. *Marine Georesources & Geotechnology*, 36(1):83-90. https://doi.org/10.1080/1064119x.2017.1285381

Zhang J, Wang H, Huang HW, et al., 2017. System reliability analysis of soil slopes stabilized with piles. *Engineering Geology*, 229:45-52. https://doi.org/10.1016/j.enggeo.2017.09.009

Zheng G, Liu JJ, Lei HY, et al., 2017. Improvement of very soft ground by a high-efficiency vacuum preloading method: a case study. *Marine Georesources & Geotechnology*, 35(5): 631-642. https://doi.org/10.1080/1064119X.2016.1215363

Zhou H, Liu HL, Zha YH, et al., 2017. A general semi-analytical solution for consolidation around an expanded cylindrical and spherical cavity in modified cam clay. *Computers and Geotechnics*, 91:71-81. https://doi.org/10.1016/j.compgeo.2017.07.005

Zou SF, Li JZ, Xie XY, 2018. A semi-analytical solution for one-dimensional elasto-viscoplastic consolidation of layered soft clay. *Applied Clay Science*, 153:9-15. https://doi.org/10.1016/j.clay.2017.11.04

## 中文概要

**题　目：考虑土体参数不确定性的软土地基塑料排水板最优化设计**

**目　的：**塑料排水板能够有效加速固结过程，因此被广泛应用于软土地基处理。然而，相关规范只给出了塑料排水板的间距和长度的取值范围，没有给出最优设计。本文旨在通过考虑土体参数不确定性、施工造价和设计要求三个方面，提出塑料排水板的最优设计。

**创新点：**1. 通过蒙特卡罗方法求解固结度的信噪比，得到不同设计的鲁棒性；2. 讨论各种因素对最优设计的影响。

**方　法：**1. 通过理论分析，推导出总固结度鲁棒性的计算公式；2. 通过定义不同设计组合，讨论不同噪声参数，并运用蒙特卡罗模拟，得到满足要求的所有设计情况的鲁棒性；3. 分析其他因素（如固结时间和固结度等）对最优设计的影响，并讨论参数变异性和相关性对结果的影响。

**结　论：**1. 基于鲁棒性分析，得到了塑料排水板的最优设计方法。2. 在低造价条件下，固结度、固结时间和塑料排水板布置形式对最优设计存在影响；当造价足够高时，该影响可以忽略。3. 参数变异性和相关性对结果存在影响；如果低估了参数的变异性，会低估最优设计的造价。

**关键词：**岩土工程鲁棒性设计；固结；塑料排水板布置形式；地基处理